J MATER SCI **41** (2006) 437–443

Temperature effects on the fatigue of highly filled PMMA

OKITE OBAKPONOVWE, J. G. WILLIAMS
Department of Mechanical Engineering, Imperial College London, SW7 2BX, United Kingdom

Published online: January 2006

The modulus and fracture toughness of an ATH-filled PMMA composite are determined as a function of temperature. The modulus can be modelled as a series addition of the two phases, giving a decreasing modulus with temperature tending to zero at 110°C. The K_{1C} value remains constant. Fatigue crack growth data in the form of *da/dN* versus *K* were obtained as a function of temperature and modelled using the Paris Law. The power index remained constant at 7.5, but the coefficient had a maximum at 50°C. It is suggested that this arises from microcracks generated by interparticle thermal stresses which are shown to have a maximum at the same temperature (50°C). A two-stage zone fatigue crack growth model was also applied to the data and gave a damage stress which correlated with the thermal stress and suggested a criterion based on achieving a constant energy per unit area.

1. Introduction

Particle filled polymer composites are widely used in kitchens and bathrooms, as both durable work surfaces and in the fabrication of sinks and basins. The addition of the second phase (ATH filler) increases the material's stiffness and aesthetic properties, i.e. texture and appearance (see [1]). Generally the mechanical performance is good, but in these applications, the materials are often subjected to thermal cycling which occurs around stove cut-outs in kitchens and in sinks subjected to alternating flows of hot and cold water. In both cases, the temperature cycles give rise to stress cycles and this in turn can lead to the propagation of fatigue cracks. It is not clear, a priori, if the material is damaged by temperature cycling or if the crack growth is simply due to the stress generated at various temperatures. To clarify this issue, some conventional fatigue crack propagation tests were performed to measure the crack propagation rate, *da/dN*, for a range of constant temperatures which covered the operating range [1].

2. Materials and experiments

The material used is a lightly cross-linked PMMA filled with about 40–50% by volume of Alumina Trihydrate (ATH) particles in the 2–10 μm average size range which occur as agglomerates of 40–50 μm. The 12.5 mm thick sheets were made by a continuous casting process with slow cooling to minimise warping and residual stresses [1]. Preliminary tests were performed by measuring elastic modulus in the 0–100°C temperature range in both simple tension (ST) and three point bend (3PB) testing. The results are presented in Fig. 1. The PMMA matrix has a modulus of about 3 GPa at 20°C and a glass transition temperature of 110°C with a linear dependence on temperature [3]. The behaviour shown in Fig. 1 may be modelled as a unit cell with a volume fraction, V, of filler of modulus E_f in series with (1-V) of polymer E_p as shown in Fig. 2. The filler is assumed to be much stiffer than the polymer so that it constraints the polymer in the transverse directions. Thus for an applied stress σ the strain in the polymer is,

$$\varepsilon_p = \frac{(1-V)}{E_p} \cdot F(\nu)\,\sigma, \qquad F(\nu) = \frac{(1+\nu)(1-2\nu)}{(1-\nu)}$$

where ν is the Poisson's ratio and,

$$E_p = E_0 \left(\frac{T_g - T}{T_g - T_0} \right)$$

E_0 is the polymer modulus at T_0 and T_g is the glass transition temperature, i.e. $T_0 = 20$°C, $E_0 = 3$ GPa and $T_g = 110$°C. E_f is not known but it is assumed to be high (>100 GPa) and independent of T and the strain in the

0022-2461
DOI: 10.1007/s10853-005-2471-0

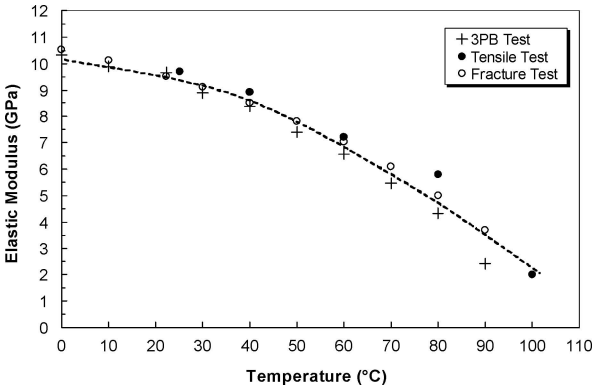

Figure 1 Elastic modulus against temperature comparing results from 3-Point bend, tensile and fracture tests.

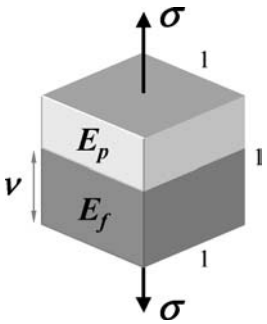

Figure 2 Unit cell of polymer and filler in series.

filler is given by,

$$\varepsilon_f = \frac{V\sigma}{E_f}$$

Thus for the unit cell the overall strain is given by,

$$\varepsilon_a = \frac{\sigma}{E_c} = \varepsilon_p + \varepsilon_f$$

where E_c is the composite modulus. Substituting for ε_p, ε_f and E_p, we have,

$$E_c = \left(\frac{E_f}{V}\right) \times \frac{(T_g - T)}{\left[\left(\frac{1-V}{V}\right)\frac{E_f}{E_0} \cdot F(\nu)(T_g - T_0) + T_g - T\right]} \quad (1)$$

The data in Fig. 1 may be fitted by

$$E_c = 18\left(\frac{110 - T}{188 - T}\right) \text{ GPa} \quad (2)$$

and the line is shown in Fig. 1. From Equation 1 we have,

$$\frac{E_f}{V} = 18\,\text{GPa}$$

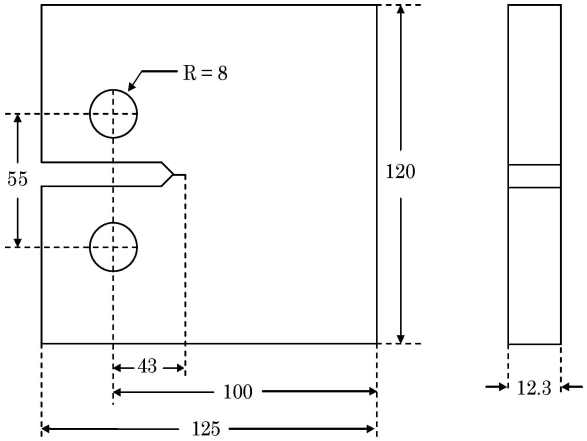

Figure 3 CT specimen configuration (all dimensions in mm).

and

$$\left(\frac{1-V}{V}\right)\frac{E_f}{E_0} \cdot F(\nu)(T_g - T_0) + T_g = 180°\text{C}$$

and on substituting for the polymer values and $\nu = 0.3$ we have,

$$V = 0.78 \quad \text{and} \quad E_f = 14\,\text{GPa}$$

The volume fraction of filler is about 0.5 so these numbers suggest that the filler is mostly in agglomerates giving an effective volume fraction of 0.78 and the rather low modulus of 14 GPa.

The low rate fracture toughness was evaluated using the ISO standard for determining K_{IC} and G_{IC} for polymers [4]. The compact tension (CT) geometry shown in Fig. 3 was convenient since the thickness of the sheet could be used as the thickness of the specimen.

The tests were conducted using a screw-driven Instron machine at 1 mm/min, and the values for K_{IC} at initiation are given by:

$$K_{IC} = f\left(\frac{a}{w}\right)\frac{F}{b\sqrt{W}} \quad (3)$$

where F is the load, f a calibration factor, b the thickness, and W the width [4]. The temperature was controlled by testing the specimen within a temperature cabinet, and was determined by inserting thermocouples into small holes drilled to the centre, along the specimen thickness. Fig. 3 shows the results for K_{IC} as a function of temperature and it remains remarkably constant at 2 MPa$\sqrt{\text{m}}$ over this range. The load deflection curves were linear and G_{IC} was found from the area under the curve, i.e. the energy. E, K_{IC} and G_{IC} are related via,

$$E = \frac{K_{IC}^2}{G_{IC}} \quad (4)$$

Thus E could be found, and the values (also shown in Fig. 1) agree closely with the values from 3PB and ST.

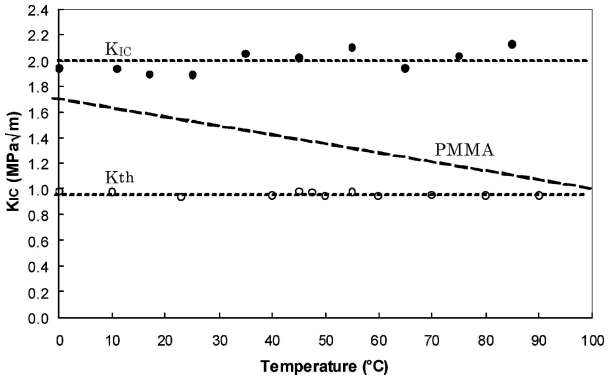

Figure 4 K_{IC} and K_{th} as a function of temperature for the filled polymer.

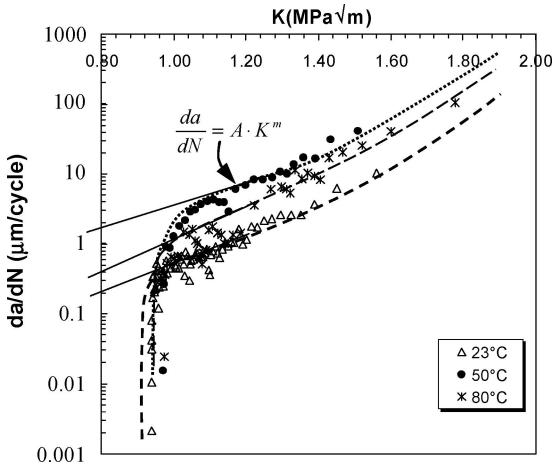

Figure 5 The effect of temperature on the fatigue growth rate curves.

Since E decreases and K_{IC} is constant, G_{IC} increases with temperature from 402 J/m^2 at 20°C to 1000 J/m^2 at 80°C. The broken line in Fig. 4 that represents PMMA [3, 5] shows a decrease in K_{IC}. The equivalent values of G_{IC} are constant at about 1000 J/m^2.

3. Fatigue tests

The fatigue tests were performed according to the ISO protocol for the fatigue testing of polymers [5], and employed the CT specimen and a temperature cabinet. The tests were conducted at a constant load amplitude and frequency of 5 Hz. Under these conditions K increases as the crack grows and hence the crack growth rate, da/dN, also increases. The growth was stable and hence da/dN could be determined over most of the growth by differentiating the a-N data. Thus da/dN as a function of K could be found. The crack length was measured using a thin metal foil gauge and a Fractomat unit. Checks were made by taking concurrent optical measurements on some specimens which confirmed the gauge values. Readings were also taken on both sides of the specimens in some cases and in general the two readings agreed confirming axial loading and uniform crack growth/progression across the thickness of the specimen. The polymer protocol thus appeared to work well even though the material was much stiffer than typical polymers. A load ratio (R) of 0.1 was employed in the tests. Fig. 5 shows three typical curves of da/dN versus K on a log-linear basis and lines drawn to fit the Paris Law,

$$\frac{da}{dN} = A\left(\frac{K}{K_0}\right)^m \tag{5}$$

A and m are constants,

$$K_0 = 1\ \text{MPa}\sqrt{m}$$

There are well defined threshold values K_{th} (also shown in Fig. 4), which are constant at about 0.96 MPa$\sqrt{\text{m}}$. The slope m is also approximately constant at 7.5, but it is noticeable that the data at 50°C is higher than at 23 and 80°C. This is reflected in the values of A which are shown in Fig. 6, and have a distinct maximum at about 50°C. This is a somewhat unexpected result since K_{IC}, K_{th} and m are independent of temperature. The values of A, m, K_{IC} and K_{th} for all temperatures are listed in Table I.

4. Discussion

A possible explanation for the peak in fatigue crack growth rate at 50°C is the generation of interparticle stresses with changing temperature.

There is a very large difference between the thermal expansion coefficients of the polymer and the filler so that a temperature change will induce a stress in the constrained

TABLE I

Temp. (°C)	A (μm/cycle)	m	K_{th} (Mpa$\sqrt{\text{m}}$)	K_c (Mpa$\sqrt{\text{m}}$)	r_c (μm)	$\alpha\sigma_c$ (MPa)	σ_T (MPa)	R_a (μm)
10	0.27	6.9	0.98	1.94	3	161	10.2	29
23	0.34	7.4	0.93	1.93	5	128	14.6	38
40	0.69	6.1	0.95	1.89	12	84	17.9	50
45	1.1	9.0	0.98	1.89	19	67	18.2	–
50	1.4	7.9	0.95	2.05	28	55	18.4	–
55	1.3	7.8	0.98	2.02	22	62	18.2	–
60	1.1	6.8	0.94	2.10	18	69	17.9	46
70	0.76	7.7	0.96	1.94	12	86	16.3	67
80	0.45	7.5	0.95	2.03	7	110	13.8	60
90	0.13	7.6	0.95	2.13	5	160	10.2	73
Average		7.5	0.96	2.00				

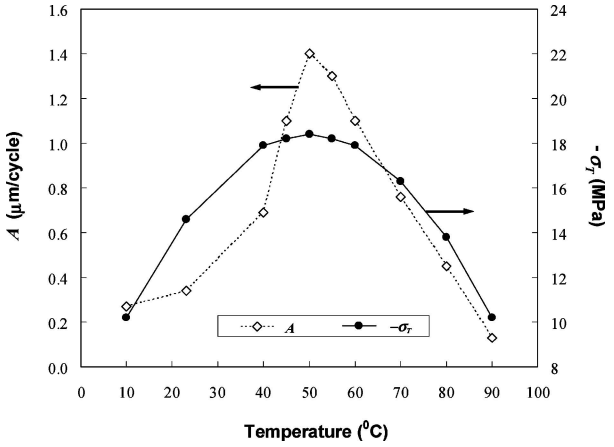

Figure 6 A and thermal stress as a function of temperature.

polymer layer, shown in Fig. 2, given by,

$$\sigma_T = \frac{E}{1-\nu} \cdot \Delta\alpha \cdot \Delta T \tag{6}$$

where $\Delta\alpha$ is the difference in coefficients of thermal expansion.

When the material is manufactured it solidifies at T_g and then cools down to room temperature and, since the contraction of the polymer is constrained, a tensile stress is set up. Since $\frac{E}{1-\nu} \approx 4\,\text{GPa}$, $\Delta\alpha \approx 10^{-4}{}^{\circ}\text{C}^{-1}$ (this is the polymer value and likely to be very much greater than that of the particles), and $\Delta T = 100^{\circ}\text{C}$ giving $\sigma_T = 40$ MPa. Annealing processes and visco-elastic relaxation will greatly reduce this value and over a long period it would tend to zero. A further complication is the absorption of water which causes swelling of the polymer and negative values of σ_T. Thus it is difficult to be sure of the σ_T value at ambient temperature. However, we may compute the change in σ_T when the temperature is changed and this is given by,

$$\sigma_T = \frac{-E_p}{1-\nu} \cdot \Delta\alpha \cdot \left(T - \bar{T}\right)$$

where $\bar{T}$ is the temperature at which $\sigma_T = 0$. Substituting for E_p we have

$$\sigma_T = \frac{-E_0 \cdot \Delta\alpha}{1-\nu} \cdot \left(\frac{T_g - T}{T_g - T_0}\right) \cdot \left(T - \bar{T}\right) \tag{7}$$

This function has a maximum at $\hat{T} = \frac{T_g + \bar{T}}{2}$ and if we assume that the peak in A at 50°C is a consequence of σ_T then putting $\hat{T} = 50^{\circ}\text{C}$ we have $\bar{T} = -10^{\circ}\text{C}$. Thus $\sigma_T = 0$ at $T = -10^{\circ}\text{C}$ and $\sigma_T = -14$ MPa at $T = 20^{\circ}\text{C}$, ambient temperature. This may arise from water absorption, as previously mentioned, or be a consequence of thermal conditioning of the material. The values of $-\sigma_T$ are shown together with A in Fig. 6 and suggest a correlation. The mechanism is difficult to define using the Paris Law since it is an empirical relationship with no

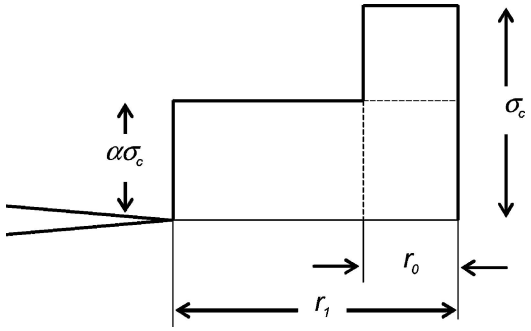

Figure 7 Two stage zone model.

basic mechanism. An alternative model of fatigue crack growth was suggested in [5] and [7] in which a two-stage Dugdale zone at the tip of the crack was used as shown in Fig. 7. Here a local stress of σ_C is proposed which is reduced to $\alpha\sigma_C$ (α is a constant factor here and not the coefficient of thermal expansion) on cycling. In the steady state the two stage zone is formed and the crack moves forward $r_0 \equiv da/dN$ in each cycle. The fatigue crack propagation law then becomes,

$$\frac{da}{dN} = \frac{r_c}{(1-\alpha)^2}\left[\left(\frac{K}{K_c}\right)^2 - \alpha\right], \quad r_c = \frac{\pi}{8}\left(\frac{K_c}{\sigma_c}\right)^2 \tag{8}$$

(some details of the derivation are given in the appendix).

This model has the advantage that it describes the threshold phenomena since at $da/dN = 0$.

$$K = K_{th} = \sqrt{\alpha} K_c$$

and hence for this material $\alpha = 0.23$. If the two models are fitted to the data to match the slope and value (see appendix for details) they agree closely for the post threshold values and, for the data here, in the range 1 MPa$\sqrt{\text{m}} < K < 1.5$ MPa$\sqrt{\text{m}}$. Using $m = 7.5$, $\alpha = 0.23$ and $K_C = 2$ MPa$\sqrt{\text{m}}$ there is an equivalence between A and r_c given by,

$$A = 0.06\, r_c \tag{9}$$

Fig. 8 gives the $T = 23^{\circ}\text{C}$ data plotted in accordance to Equation 8, showing the threshold and for which $r_c = 5$ μm. It can be seen that for $K^2 > 1.8(\text{MPa}\sqrt{\text{m}})^2$, da/dN increases more rapidly than the model suggesting a change in mechanism [7]. Similar effects were reported for several polymers, including PMMA, in [7]. Fig. 9 shows A plotted against r_c for the different temperatures and Equation 9 which indicates that the two stage zone model is a sensible fit to the data.

It is possible to determine $\alpha\sigma_C$, the damage stress, for each temperature and these are listed together with r_c in Table I. This may then be compared with σ_T from Equation 7 ($\bar{T} = -10^{\circ}\text{C}$) and the values are also given in

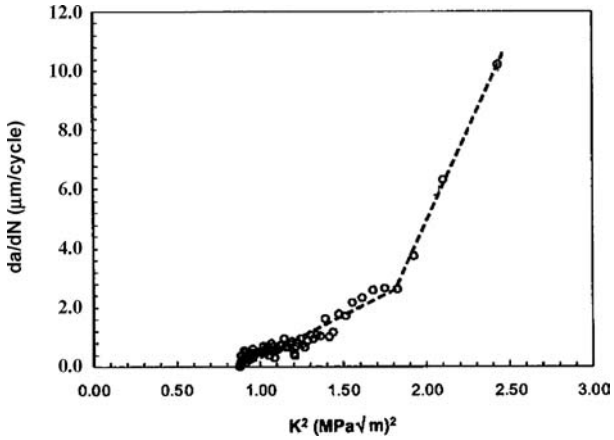

Figure 8 $T = 23^{\circ}$C data plotted in accordance to Equation 7, the two stage zone model.

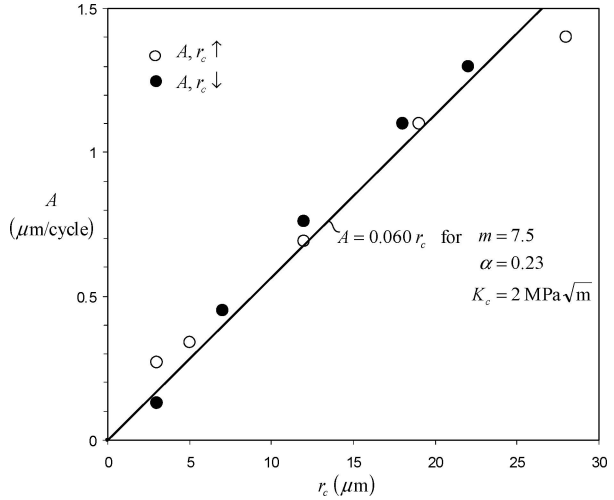

Figure 9 A comparison of A from the Paris Law and r_c from the two stage zone model.

Table I. There is clearly a strong inverse correlation with these stresses which is remarkable considering that they are derived completely separately.

A possible source of the correlation is the damage process around the crack tip. $\alpha\sigma_C$ defines the input stress to produce this while σ_T is the contribution to damage via the thermal stresses. If we assume flaw sizes of c_1 for the fatigue damage and c_2 for the thermal damage then summing G_c values at failure we have,

$$(\alpha\sigma_C)^2\,\pi c_1 + \sigma_T^2 \pi c_2 = (\alpha\sigma_0)^2\,\pi c_1 = E\alpha G_{1C} = \alpha K_{1C}^2 \qquad (10)$$

i.e.

$$(\alpha\sigma_C)^2 = (\alpha\sigma_0)^2 - \left(\frac{c_2}{c_1}\right)\sigma_T^2$$

where $\alpha\sigma_0$ is the damage stress in the absence of σ_T and is assumed to be constant here. Fig. 9 shows the data plotted in this form and both r_c increasing ($T < 50^{\circ}$C) and

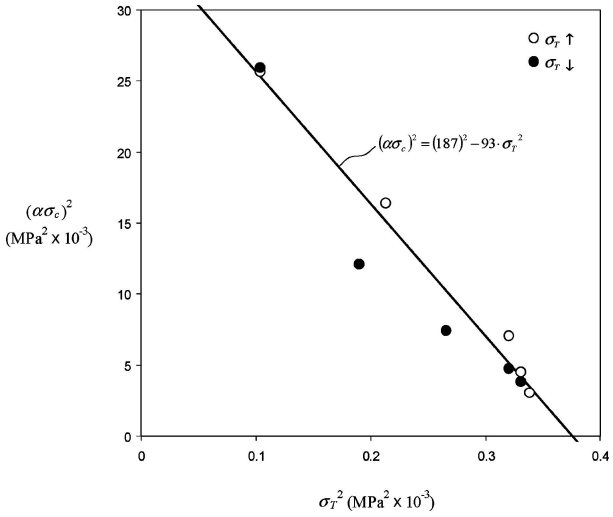

Figure 10 Fatigue damage stress, $\alpha\sigma_c$ as a function of interparticle thermal stress σ_T.

decreasing ($T > 50^{\circ}$C) fit the relationship well giving,

$$\frac{c_2}{c_1} = 93 \quad \text{and} \quad \alpha\sigma_0 = 187\,\text{MPa}$$

The value of σ_c is given by $\sigma_c^2 = \frac{\pi}{8}\frac{K_c^2}{r_c}$ and when $\sigma_T = 0$, $\sigma_c = \sigma_0 = 813$ MPa. This is a high value and compares with 750 MPa found for PMMA in [7]. It is believed to represent the local stress at the tip of the zone while $\alpha\sigma_0$ is that in the damaged region. c_2/c_1 describes the ratio of the length scales of the two damage processes.

A value of c_1 may be deduced from Equation 10 since,

$$c_1 = \frac{\alpha}{\pi}\frac{K_{IC}^2}{(\alpha\sigma_0)^2} = 8\,\mu\text{m}$$

which is within the range of the particle sizes, 1–10 μm. The value of c_2 is thus 740 μm which is 15 times the agglomerate size of 50 μm.

The fracture surfaces were rough [2] and micrographs showed a white and rugged surface. They were evaluated with a Talysurf probe to determine the arithmetic mean of the roughness R_a. The average values for some of the temperatures are given in Table I and are about 60 μm which is close to the agglomerate size.

It would also be expected that surface treatment of the particles would be influential. This would arise via σ_T since the derivation assumes perfect adhesion so that an adhesion inhibitor would decrease σ_T and hence decrease A in fatigue. However, surface properties would affect dispersion and hence c_2, and we would expect that an adhesion inhibitor would decrease c_2, and once again decrease A. Some very limited results were obtained using two materials with adhesion promoters which did, indeed, give peaks in A at about 60°C (as opposed to 50°C) which increased by factor of 5 and 9 confirming that high adhesion made things worse for fatigue resistance though the mechanism by which this occurred could not be ascertained.

A material with an adhesion inhibitor did, however, also give an increase in A of about a factor of 3 contradicting the expectations. A small (30%) decrease in A was found for a material with no particle surface treatment. These are very limited results and require further investigation to evaluate the ideas about mechanisms.

On a final point, some specimens were precycled from room temperature to 100°C and then the modulus and A were determined at 23°C after different numbers of cycles. This was to explore the notion that temperature cycling, rather than stress cycling, gives rise to damage. It was found that E decreased by about 4% in the first cycle but remained unchanged up to 150 cycles. A and m were unchanged by the thermal precycling. These results confirm that the thermal fatigue observed in these materials arise from the thermally induced cyclic stresses and that there is no contribution to damage from the thermal cycling itself. The thermal stresses around the particles, however, do affect behaviour because they cause damage, though not by cycling.

5. Conclusions

It has been shown that this highly filled and stiff composite can be tested for fatigue crack propagation using methods developed for polymers. Such methods can also be used over a range of temperatures. For the temperatures of interest the material showed a marked peak in fatigue propagation rate at about 50°C. By contrast the threshold K value and final fracture values remained constant with temperature.

Interparticle thermal stresses may be estimated and, by fixing one parameter, be shown to maximise at the same temperature. This comes about because of the decrease of modulus with temperature and the corresponding rise in thermal strain. When a two-stage zone damage model is employed a damage stress may be found for each temperature and gives a minimum at 50°C. An additive model of energy release rates predicts a constant total damage stress and a ratio of length scales for fatigue and thermal damage. The fatigue length scale correlates with the particle size but the thermal damage value is much higher than the agglomerate size.

There is some measure of speculation in the ideas presented but they do show promise in describing the rather complex behaviour observed.

Appendix: The two stage zone model

The model is based on defining the zone lengths, r_0 and r_0, in terms of r given by,

$$r = \frac{\pi}{8}\frac{K^2}{\sigma_c^2}$$

and from equilibrium we have,

$$\sqrt{r} = \alpha\sqrt{r_1} + (1-\alpha)\sqrt{r_0} \tag{A.1}$$

The crack opening displacement is given by,

$$\delta = \frac{\pi}{8}\frac{\sigma_c}{E}\cdot r_1\left[\alpha + (1-\alpha)F(\zeta)\right]$$

where $\zeta^2 = \frac{r_0}{r_1}$, and $F(\zeta) = \zeta + \frac{1}{2}(1-\zeta^2)\ln(\frac{1+\zeta}{1-\zeta})$

For $\zeta \ll 1$, i.e. $r_0 \ll r_1$, $F(\zeta) \approx 2\zeta$ and if one assumes that failure occurs when $\delta = \delta_c$, the value in the undamaged state then,

$$\delta = \delta_c = \frac{\pi}{8}\frac{\sigma_c}{E}\cdot r_c = \frac{\pi}{8}\frac{\sigma_c}{E}\cdot r_1\left[\alpha + 2(1-\alpha)\sqrt{\frac{r_0}{r_1}}\right]$$

i.e.

$$r_c = \alpha r_1 + 2(1-\alpha)\sqrt{r_0}\cdot\sqrt{r_1} \tag{A.2}$$

Substituting for r_1 from Equation A.1 we have

$$r_0 = \frac{(r - ar_c)}{(1-\alpha)^2}$$

and since it is assumed that $r_0 \equiv \frac{da}{dN}$ we have,

$$r_0 \equiv \frac{da}{dN} = \frac{r_c}{(1-\alpha)^2}\left[\left(\frac{K}{K_c}\right)^2 - \alpha\right] \tag{A.3}$$

It should be noted that fracture is defined by

$$G_c = \frac{K_c^2}{E} = \delta_c\sigma_c$$

without fatigue but for fatigue,

$$G_c = \delta_c\alpha\sigma_c \tag{A.4}$$

If Equation A.3 is matched with both slope and value with the Paris Law,

$$\frac{da}{dN} = A\left(\frac{K}{K_0}\right)^m, \quad K_0 = 1\,\text{MPa}\sqrt{\text{m}}$$

then

$$\frac{d}{dK}\left(\frac{da}{dN}\right) = \frac{2\bar{K}\cdot r_c}{(1-\alpha)^2K_c^2} = Am\frac{\bar{K}^{m-1}}{K_0^m}$$

and

$$\frac{da}{dN} = \frac{r_c}{(1-\alpha)^2}\left[\left(\frac{\bar{K}}{K_c}\right)^2 - \alpha\right] = A\left(\frac{\bar{K}}{K_0}\right)^m$$

where K is the value of K at the matching point. Thus,

$$\left(\bar{K}/K_c\right)^2 = \left(\frac{m\alpha}{m-2}\right) \tag{A.5}$$

and

$$\frac{r_c}{A} = \left(\frac{K_c}{K_0}\right)^m \cdot \frac{m}{2}(1-\alpha)^2 \left(\frac{m\alpha}{m-2}\right)^{\frac{m}{2}-1} \quad \text{(A.6)}$$

For this set of data $m = 7.5$, $\alpha = 0.23$ and $\frac{K_1}{K_0} = 2$ so that,

$$\frac{\bar{K}}{K_c} = 0.56 \quad \text{and} \quad \frac{A}{r_c} = 0.06.$$

Acknowledgments

The authors wish to thank DuPont for the supply of the material and financial support.

References

1. US Patent 3,847,865 Nov. 12 (1974) "Use of Aluminum Trihydrate in a Poly Methyl Methacrylate Article.
2. O. OBAKPONOVWE, PhD Thesis "Temperature Effects in Fatigue of Alumina-Filled PMMA," Imperial College London (Aug. 2003).
3. G. P. MARSHAL, L. H. COUTTS and J. G. WILLIAMS, *J. Mater. Sci.* **9** (1974) 1409.
4. ISO 13586 (2000) "Plastics—Determination of Fracture Toughness (G_C and K_C)—an LEFM approach.
5. J. G. WILLIAMS, "Fracture Mechanics of Polymers" (Ellis Horwood Ltd. 1987).
6. ISO 15850 (2002) "A Protocol for Tension-tension Fatigue Crack Propagation Testing in Plastics".
7. J. G. WILLIAMS, *J. Mater. Sci.* **12** (1977) 2525.

Received 12 January
and accepted 24 May 2005